Cement hydration: the role of adsorption and crystal growth

G. Artioli*[1] and J. W. Bullard[2]

[1] Università degli Studi di Padova, Dipartimento di Geoscienze e Centro Interdipartimentale di Ricerca per lo Studio dei Materiali Cementizi e dei Leganti Idraulici (CIRCe), Via Gradenigo, 6-35131, Padova, Italy

[2] Materials and Construction Research Division National Institute of Standards and Technology 100 Bureau Drive, Gaithersburg, MD, USA

Portland cement is a fundamental structural and binding material for industry and society. Its structural and physical properties at different scales show a complexity that can presently be barely managed through experimental and computational methods. State of the art problems and trends in cement studies will be briefly assessed from the point of view of the processes at the molecular scale.

1 Introduction to inorganic binding materials

Cements based on Portland-type clinkers, mortars (pastes and plasters prepared with fine aggregates), and other inorganic binders form an important class of construction materials: they are all supplied as powders and when mixed with water they form a fluid mass (paste) that can be shaped, moulded, added to other components, or attached to the surface of other materials. The paste then hardens spontaneously at normal environmental conditions.

Binding materials are used in buildings with the aim of (a) making structural elements for constructions, (b) increasing the mechanical resistance of the construction by linking the structural and architectural elements, (c) increasing water resistance and protecting masonry surfaces from environmental degradation, and (d) preparing substrates for artwork and decorative purposes. Excluding last century's binders and adhesives based on organic polymers, the binders used in antiquity are inorganic compounds based on carbonates (calcite, dolomite), sulphates (gypsum) and alumino-silicates (cements).

Starting from the properties of classical Roman materials (pozzolanic lime-based mortars) the search for optimal hydraulic binders was actively pursued in several countries in the first half of the 19th century [1,2], the most successful being those of J. Smeaton and J. Parker in Britain, and those of L.J. Vicat in France. The modern cement formulation is commonly traced back to the three-stages process of J. Aspdin (1824), who described his product as Portland cement, because of its similitude with the reputed Portland limestone, favoured among British builders for its quality and durability [1].

The clinker is the reactive product formed by cooling a limestone and clay mixture from a high processing temperature (1450 °C) within a kiln. The kiln temperature is high enough to cause partial fusion, with reacted molten material lumping into nodules that are partly crystalline and partly liquid. Upon cooling, the liquid phase crystallizes and the whole material becomes highly reactive with water. The basic four-phase composition of the clinker is reported in Table 1, though the real situation is far more complicated by the existence of several polymorphs for each phase, and by compositional deviation from the indicated stoichiometry. The basic chemical composition of Portland cement is shown in figure 1, where it is evident that the composition of the two major phases (alite and belite) lie on the $CaO-SiO_2$ join as a result of the lime-silica reaction.

The main characteristics of modern Portland clinkers are actually derived from the use of rotary kilns in place of the historical shaft kilns, a technical development that also allows continuous production in place of the batch process. The carefully controlled initial formulation of calcareous and argillaceous components, together with

*Corresponding author: e-mail: gilberto.artioli@unipd.it

Table 1 Main phases of ordinary Portland clinkers [3].

Phase	composition	cement notation	wt% range
alite	$Ca_3SiO_5 = 3CaO·SiO_2 =$ tricalcium silicate	C3S	50–70
belite	$Ca_2SiO_4 = 2CaO·SiO_2 =$ dicalcium silicate	C2S	15–30
aluminate	$Ca_3Al_2O_6 = 3CaO·Al_2O_3 =$ tricalcium aluminate	C3A	5–10
ferrite	$Ca_2AlFeO_5 =$ tetracalcium aluminoferrite	C4AF	5–15
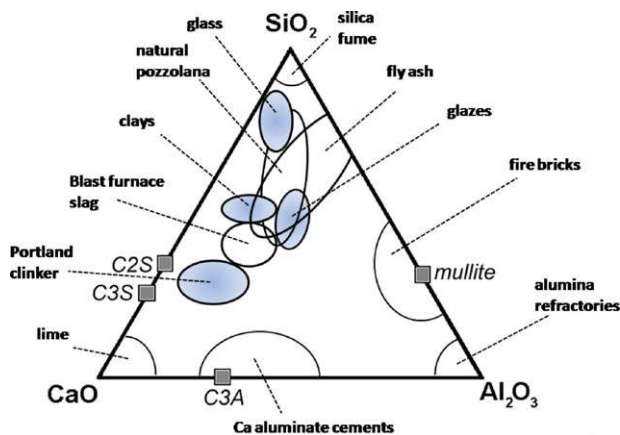
Fig. 1 Ternary CaO-Al_2O_3-SiO_2 diagram showing the composition of major clinker phases and general compositions of commercial cements.

the use of the rotary kiln that provides a long residence time at high temperature and continuous mixing, favors (a) the minimization of the amount of un-reacted lime, (b) the maximization of the alite/belite ratio, and (c) the appropriate crystal size of the mineral components, commonly in the range of 10 μm to 40 μm. Modern clinkers contain about 60% to 65% by mass of C3S, and less than 2% of un-reacted free lime. The standard reaction properties of modern Portland clinker are essentially due to a high alite/belite ratio and to careful control of the grinding of the clinker into a fine powder.

1.1 Cement hydration: The nature of the reactions The very reactive Portland cement clinker powder can be mixed with water to produce a final hardened material through a series of complex reactions, the so-called hydration process, involving dissolution of the crystal phases, surface reactions, gel formation, precipitation of new phases, and textural changes [3,4]. The different crystal phases present in the clinker have very different reactivities, C3A having the highest and C2S the lowest. As a matter of fact, C3A is so exothermally reactive that it can cause unwanted rapid setting of the paste (flash set), with concurrent loss of workability. Therefore, a calcium sulphate material (commonly gypsum, but also bassanite and/or soluble anhydrite) is usually interground with the clinker in the amount of about 4% to 8% by mass as a set-controlling agent.

The finely powdered mixture of clinker and gypsum is marketed as standard Portland cement (PC, often called ordinary Portland cement), which is then mixed with water. The mass ratio of water to cement, w/c, typically ranges from 0.3 to 0.5, although sufficient water to fully react with cement would require w/c to be about 0.38 or greater. When an aggregate material is added to the paste we have mortar (fine aggregate, such as sand with grain size below 1 mm) or concrete (fine and coarse aggregate, such as coarse sands or gravel). They both can be considered cement composites, with the aggregate having the roles of imparting greater stiffness and of reducing the formation of fractures during the shrinkage that accompanies the hydration and hardening. The aggregate may be composed of any type of loose or ground rock, and it is assumed not to react with the cement paste (hence it is inappropriately called the inert component), though this is not necessarily the case.

Upon mixing with water the clinker phases react at different rates to produce a collection of hydration product phases such as ettringite ($Ca_6Al_2(SO_4)_3(OH)_{12}·26H_2O$), monosulphoaluminate ($Ca_4Al_2(SO_4)O_6·12H_2O$), portlandite ($Ca(OH)_2$) and amorphous calcium silicate hydrate (C-S-H), which are the phases forming the interlocked gridwork of the material and producing high mechanical resistance. The completion of the hydration process may take weeks, months, or even years depending on the crystal size, the crystal defects and polymorphism of the phases, the porosity of the paste, the environmental conditions, etc. With time portlandite may eventually
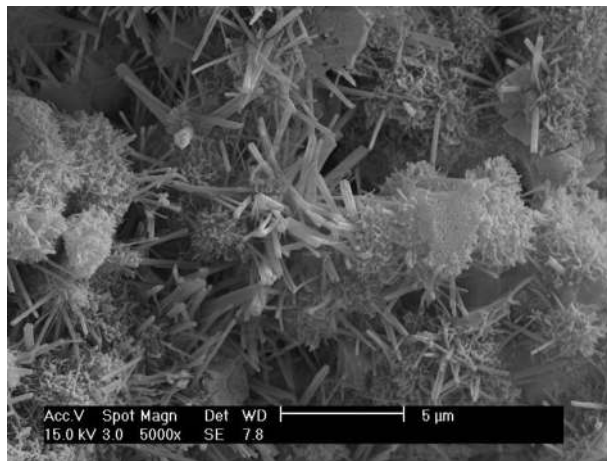
Fig. 2 ESEM figure of ettringite prismatic crystals growing on the clinker grains. (Image courtesy of Central Analytical Laboratory, Mapei Spa).
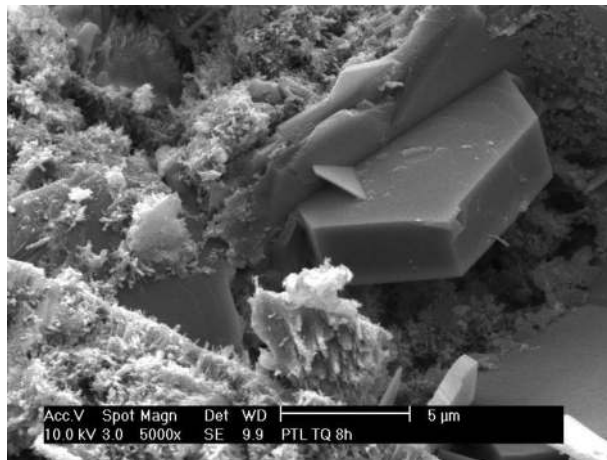

Fig. 3 ESEM figure of C-S-H and a well developed portlandite crystal growing on the clinker grains. (Image courtesy of Central Analytical Laboratory, Mapei Spa).

convert into calcite through a carbonation reaction with atmospheric carbon dioxide, so that abundant calcite is found in old cements. Figures 2 and 3 show environmental scanning electron microscope (ESEM) evidence of the growth of ettringite, C-S-H, and portlandite at different times on the surface of the clinker grains.

2 Properties of cement

Strength development is related to the degree of hydration and to the speed of the process. When the hydration process is intentionally accelerated by increasing the curing temperature there is usually a corresponding loss in long term compressive strength. However, other factors that increase the hydration rate, such as using finer particle sizes, either do not cause a strength loss or may even increase the ultimate strength. Significant differences are sometimes observed in the difference between modern clinkers and those produced in the early part of the 20th century. The modern cement is required to develop high resistance to compression (over 40 MPa) within a few days of its placement, whereas cements used in the early 1900s developed high strengths (in the range 20–30 MPa) over much longer times because of their higher belite content and coarser particle sizes.

Nowadays only about 35% of the cements industrially produced for the global market are so-called "ordinary" Portland cement (PC, in the past also referred to as OPC). The remainder of the materials are special composite formulations [5,6], in which different components are added to enhance specific physico-chemical

Table 2 Main types of common and special cements..

Cement type	Portland clinker wt%	composition	properties
Portland cement (PC) [CEM I[a]]	95–100	Mixed with minor constituents	Common cements
Special cements [CEM II[a]]	65–94	Mixed with blast furnace slags, silica fume, natural or calcined pozzolans, fly ash, burnt shale, limestone	Blended cements with enhanced durability
Blast furnace cement [CEM III[a]]	5–64	Mixed with blast furnace slags	
Pozzolanic cement [CEM IV[a]]	45–89	Mixed with pozzolan, silica fume, fly ash	
Composite cement [CEM V[a]]	20–64	Mixed with blast furnace slag, pozzolan, fly ash	
High belite cements	95–100	Belite>alite obtained by fast quenching of clinker	Slow steady increase in strength, low heat production
Calcium aluminate cement (CAC) or high alumina cement (HAC)	0	Made by fusion of limestone and bauxite	Rapid increase in strength, superior sulphate resistance, resistance to high temperature
Fiber cement	95–100	Mixed with reinforcing fibers (polymeric, steel)	Crack control, reinforcement, reduction of plastic shrinkage, shotcrete applications
Cement-polymer systems	variable	OPC or HAC mixed with water-soluble polymers	Macro-defect free (MDF) materials, high compressive and flexural strength
Ultra-rapid hardening cements	85–90	$C_{11}A_7CaF_2$>20 wt%	Very rapid development of strength, jet cement applications
Expansive cements	variable	8–12 wt% anhydrite Contain $3CA \cdot CaSO_4$ (yeelemite), lime, or high-C3A	The expansive component is used to compensate OPC shrinkage

[a]Classification (UNI EN 197-1, 2007)

or mechanical properties (Table 2). The main added constituents are (a) latent hydraulic components (granulated blast furnace slags, metakaolin, Class C fly ash) having hydraulic properties that need to be activated by portlandite or hydrated lime, (b) pozzolanic aluminosilicate components (Class F fly ash, silica fume, natural pozzolan) that have no hydraulic properties and need to be activated by portlandite, and (c) nonreactive or poorly reactive components that modify the grindability of the clinker or the rheology of the paste, such as limestone powder.

Furthermore, the rheological and working properties of cement pastes are now invariably controlled with the use of chemical admixtures (water-soluble organic polymers) that allow good fluidity of the paste with lower water/cement ratio. The net result is also a lower porosity of the paste and a higher mechanical strength: high performance concrete (HPC) and high strength concrete (HSC) are made in this way and they can reach compressive strengths of over 150 MPa. Organic and inorganic additives are used to control specific properties of the mortars and cements, such as air entrainment (for a better resistance to freeze and thaw cycles), acceleration or retardation of the setting (to control the time of progressive increase in mechanical resistance), plasticity and viscosity (plasticizing or super-plasticizing effects to control the workability of the paste), and even resistance to chemical attack. Modern additives are designed for specific actions, but the concept of using additives to change the paste properties has been known for millennia. Ancient Mesoamerican and Chinese briefly mention the use of additives in recipes for lime plasters, and the Egyptians, Minoans, and Romans also used to modify the lime in mortars with a number of organic compounds including Arabic gum, animal glue, fig's milk, egg's yolk and many others in the attempt to improve the mechanical or working properties [7]. The modern range of plasticizing additives is mostly confined to polyvinylic alcohols, meta-acrylic polymers, naphthalene, poly-carboxylates, and ligno-sulphonates, and a few others though this is a very active field of research [8–10].
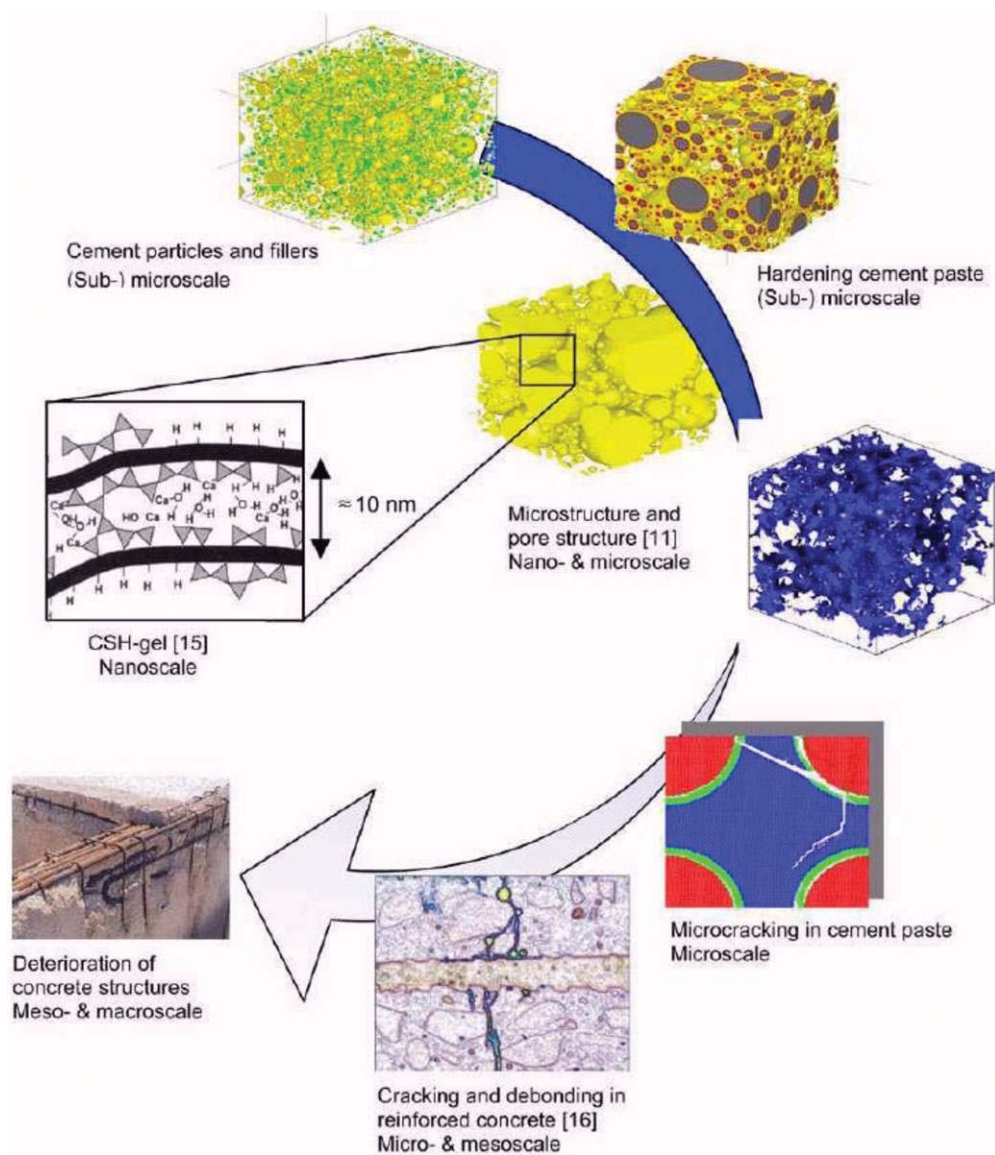
Fig. 4 The multi-scale nature of cement properties [11]. Adapted with permission from: "Modelling of cement-based systems. The alchemy of cement chemistry" by K. van Breugel, Cement and Concrete Reasearch 34, issue 9, (2004) 1661–1670. Copyright© 2004, Elsevier

Depending on the nature of the starting phases, the admixture component(s), and the environmental conditions of the hydration reactions, one or more of the occurring chemical reactions can be accelerated or inhibited, because of interference with one or more of the rate limiting steps (adsorption, surface and volume diffusion, dissolution of primary phases, nucleation and growth of secondary phases). Such manipulation can in turn affect the multiscale microstructure of the evolving cement paste (figure 4). The rheology of the cement paste, which is of great importance to manufacturers and building companies, and the mechanical resistance of the hardened cement or concrete, determining its application and durability, are critically controlled by the type and sequence of the chemical reactions occurring during the setting and hardening stages. The complexity of the system is such that the overall monitored evolution of the hydration process, typically performed by calorimetric measurements (figure 5), can be deeply affected by the change of any component. This is what makes every single cement a truly unique material.

The changes in the kinetics of the reactions can be caused by the chemistry of the solution, the crystal defects and polymorphism of the clinker phases, the nature and solubility of the calcium sulphate phases, the presence of
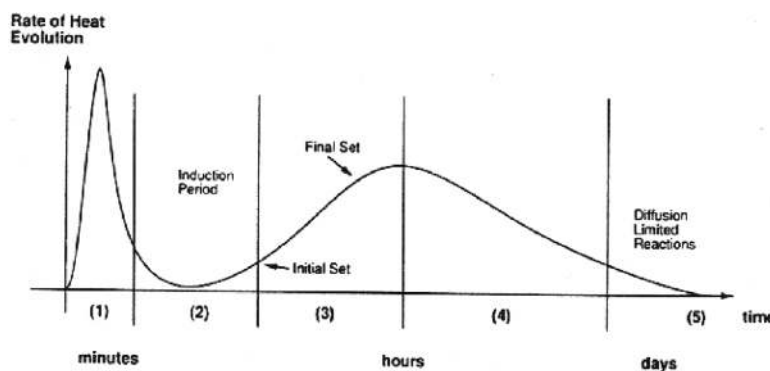
Fig. 5 Heat evolution during the hydration of a cement paste. The five steps describing the process follow the convention of Gartner et al. [4]. Reprinted with permission from: "Hydration of Portland cement" by E. M. Gartner, J. F. Young, D. A. Damidot, I. Jawed in: Structure and performance of cements-2nd Edition, J. Bensted & P. Barnes Eds., Spon Press, London-NewYork,2002, pp 57–113. Copyright©2002,Taylor&Francis Books (UK).

impurities, environmental conditions such as a temperature and humidity, and of course by any chemical additive added to the admixture.

3   Open problems

Here is a short list of pending problems involving cement systems and needing appropriate understanding at the molecular level.

The mechanisms controlling hydration. Given the complexity of the cement systems and of the reactions involved during hydration, it is no surprise that the phenomenological behaviour is mostly known and well described, though a complete interpretation of the mechanisms involved is still largely lacking. The two main models commonly invoked to explain many of the observed features of the hydration process are based on the metastable barrier layer (MBL) or on the slow dissolution step (SDS) assumptions. The MBL model implies the formation of an hydration layer at the surface of the hydrating clinker particles, which slows down the hydration process during the so-called induction (or dormant) period (i.e. period 2 in figure 5), and then becomes unstable for chemical (diffusion) or mechanical (crystallization) reasons, thus allowing the hydration to start again at later times (set period 3 in figure 5) [12,13]. This model has found some support from recent experiments based on nuclear resonance reaction analysis (NRRA, [14,15]). The SDS model on the other hand assumes that the discontinuity in the hydration rate is caused by the contrasting rates of dissolution of the clinker phases and of precipitation of the secondary phases (mainly C-S-H), which cause fluctuations in the saturation of the chemical species in solution [16–18]. The debated topic concerning the mechanism(s) causing the induction period is still fiercely discussed in the cement community. This is certainly an area of poorly understood (albeit critically important) surface processes. Details on the mechanisms and computational demands are discussed below.

The control of rheology. Another area of substantial debate is the role of crystal morphology and surface interaction between particles in determining and controlling the rheology of the cement paste [19,20]. The rheology is affected by the micro-texture of the paste, and the micro-textural evolution of the system in turn is affected by the dissolution-crystallization reactions during hydration [21,22]. Again, how the modern super-plasticizing additives operate to change the kinetics of the reactions is empirically observed but hardly modelled at a molecular level [23,24]. The organic-inorganic interaction at the surface of the hydrating particles is a key process that is still poorly investigated, though some modelling at the molecular level has been attempted [25].

The atomic and molecular structure of C-S-H. Despite a good deal of evidence in recent years indicating that the C-S-H phases have an essentially tobermoritic or jennitic structure at the nanoscale [26–28], their poor crystallinity and short range character have prevented a satisfactory structural description. How far existing structural models [29–32] can be applied to real systems is an active field of investigation. An intimate structural description of C-S-H is needed to model crystallization and growth of this major phase involved in cement set and hardening, but structural information alone is not sufficient. A number of almost untouched issues include the structural incorporation of the organic additives [33,34], the role of impurities and disorder in the long-term

durability of these phases, and the possible structural role of C-S-H in the stabilization of hazardous or toxic species.

4 The role of adsorption and crystal growth in the hydration process

The hydration process starts immediately upon wetting of the clinker by rapid reactions between alite and C3A and water:

$$C3S + 3H_2O \rightarrow 3Ca^{+2} + H_2SiO_4^{-2} + 4(OH)^- \tag{1}$$
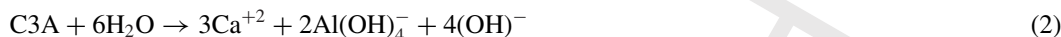
$$C3A + 6H_2O \rightarrow 3Ca^{+2} + 2Al(OH)_4^- + 4(OH)^- \tag{2}$$

These reactions have a large exothermic character (see initial peak in stage 1, figure 5), consistent with a large thermodynamic driving force for dissolution. The enthalpy of congruent dissolution of alite is -138 kJ/mol and of C3A is -248 kJ/mol, based on the reactions above [35,36]. Solution chemical analyses have furnished persuasive evidence that both C3S and C3A dissolve congruently and quite rapidly in the first seconds after wetting. In dilute suspensions of C3S, for example, the increase in silicate concentration over the first 30 s suggests that the dissolution rate may be at least $10 \ \mu mol \cdot m^{-2} \cdot s^{-1}$ [37]. In fact, Stein [38] calculated a theoretical solubility product for C3S of $K_{sp} \approx 3$, which would imply that C3S should continue to dissolve until reaching equilibrium calcium and silicate concentrations in solution of several hundred mmol/L. In fact, it is well known that C3S and alite dissolution rates decelerate very quickly while the solution is still undersaturated, by about 17 orders of magnitude with respect to the ion activity product of reaction (1) compared to the equilibrium calculation, by the end of Stage 1 [13]. The reason for slow alite dissolution while the solution is still significantly undersaturated is one of the puzzles of hydration. Possible mechanisms (i.e. MBL and SDS model) have been shortly addressed above, each one does indeed show advantages and disadvantages in explaining the experimental evidence in detail. The induction period (Stage 2, figure 5) appears to exist as a distinct stage only when chemical retarders are added, indicating a complex interplay between the C3S/C3A dissolution, the C-S-H precipitation, and the crystallization and growth of intermediate phases in the presence of gypsum (AFt and AFm phases, especially ettringite). Ettringite is known to play a critical role in controlling the rheology of the paste in the early stages of hydration, so that the interaction of the organic additives with the sulphate-containing phases is of extreme interest to develop control of the fluidity [22,23]. When alite starts rehydrating again, at the onset of stage 3 (figure 5), the reaction shows a typical autocatalytic behaviour, since the rate of hydration depends on the amount of some hydration product, essentially C-S-H. Experimental evidence, especially from microscopic techniques, indicates that the rate controlling-factor is the heterogeneous nucleation and growth of C-S-H on alite [31,39], and/or the aggregation of the C-S-H nuclei and growing particles [27,40,41]. The process can be greatly accelerated by increasing the nucleation process (for example by seeding [42]) and its kinetics is also remarkably affected by the impurities and defects present in the structure of alite, besides the intrinsic stacking and structural disorder characteristic of the C-S-H sheets. All structural models of C-S-H phases include a remarkable degree of disorder at the nanoscale [29–32], which explains the anisotropic difficult growth of the C-S-H crystals, whose morphology is variously described as frustrated sheets, crumpled foils, and other creative forms. The same structural reason is at the base of the limited crystalline growth of the natural analogues of the calcium silicate hydrates (tobermorites, gyrolite, xonotlite, afwillite, hillebrandite, foshagite, rankinite, kilchoanite, truscottite, Ca-chondrodite, etc. [43]), which are seldom found as good single crystals of reasonable size.

It is thus quite obvious that molecular adsorption, crystal nucleation and crystal growth are fundamental processes acting simultaneously in the different stages of cement hydration, and any small variation in the kinetics of these processes greatly affects the microstructural evolution of the material. The complex transformation kinetics observed between these phases [44] and the colloidal nature of C-S-H [45,46] makes the deep understanding of the real structure and microstructure of cement a substantial challenge, both from the experimental point of view (Section 6) and from the theoretical-computational point of view (Section 7).

5 Experimental challenges

A multi-scaled material such as cement (figure 4), whose physical and mechanical properties at the macroscale are closely related to its microstructure and nanostructure, can be profitably investigated by different techniques to obtain complementary information.
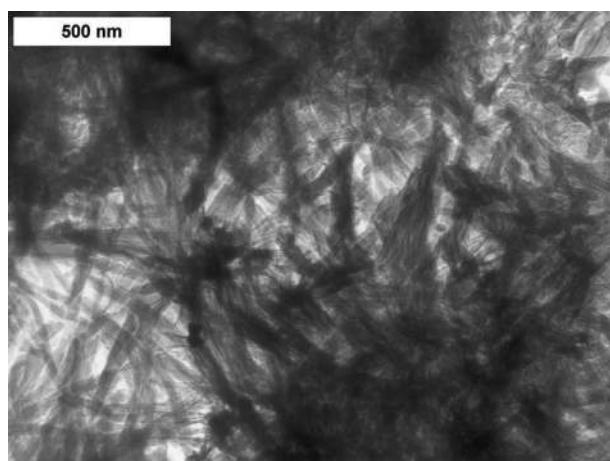
Fig. 6 Nanoscale layered organization of C-S-H phases [31]. Reprinted with permission from: "Tobermorite/jennite and tobermorite/calcium hydroxide-based models for the structure of C-S-H: applicability to hardened pastes of tricalcium silicate, Portland cement, and blends of Portland cement with blast-furnace slag, metakaolin, or silica fume" by I.G. Richardson, Cement and Concrete Research 34, issue 9 (2004) 1733–1777. Copyright© 2004, Elsevier.
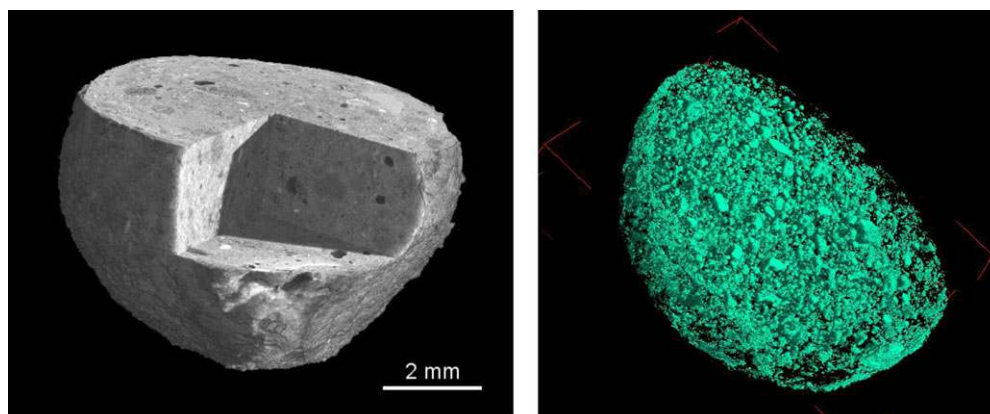

Fig. 7 X-ray absorption tomographic image of a cement pellet used for waste solidification, showing virtual sections (left), and the pore structure of the pellet extracted through analysis of the reconstructed image (right). (Images courtesy of M. Parisatto @ UNIPD).

Schematically we may identify several techniques that have been successfully employed to visualize (AFM, HR-TEM) or characterize (XRD, MAS-NMR) the structure at the atomic and molecular level. Figure 6 shows the organization of the crystalline C-S-H phases at the nanoscale within the calcium silicate hydrate gel.

The structural organization of the crystalline regions are usually derived from the single crystals of natural analogues such as 11 Å or 14 Å tobermorites and jennite [29,30], whereas the local crystallochemical arrangement is typically characterized by high resolution MAS-NMR spectroscopy [47,48]. Quantification of the crystalline phases present in the starting powder and their evolution during hydration is commonly performed by full-profile Rietveld-type analysis of the powder diffraction spectra. In situ X-ray or neutron powder diffraction is probably the optimal technique to follow the phase changes through the process [49,50], though many of the intermediate phases, especially the aluminate hydrates, do not yet have an appropriate description of their crystal structural model [51]. Imaging of the nanostructure of cement is performed by HR-TEM (figure 6) and by AFM [38] though these techniques are intrinsically invasive and generally affect the process and/or the texture of the paste. There are claims that the electron beam may induce formation of crystalline domains in the gel and/or damage in the existing structures [31]. The visualization of the unperturbed microstructure of cement may be obtained through hard X-ray tomographic techniques (figure 7).

By using fluorescence or diffraction signals for the tomographic reconstruction, it is in principle possible to map the three-dimensional distribution of the phases within the sample without any perturbation of the chemical reactions and the microstructure [52]. Present resolution of laboratory tomography is of the order of 0.5 μm, whereas with the advent of the next generation optics, nanoscale resolution should be reached at synchrotron beam lines (http://www.esrf.eu/files/Upgrade/LTS_060706.pdf). The final goal of course is to obtain simultaneously time-, space-, and phase-resolved information. These are needed to reliably assess the spatial evolution of the phases involved in the hydration process, and to fill the gap between theoretical modelling and the interpretation of the macroscopic properties.

6 Progress and challenges in computational modeling

The mechanisms of C-S-H growth are critical to understanding the development of microstructure and aiding the discovery of ways to control the rate of hydration. The qualitative understanding of the relationship between accelerated hydration and C-S-H growth is reasonable, but the quantitative relationship between and is more difficult to establish. Computational models are used to systematically vary the system parameters and understand their control on the reaction kinetics, on the nature of the products, and on the microstructure of the paste from the nanoscale [53] to the macroscale [54].

The earliest mathematical models of cement hydration kinetics focused on the hydration of a single spherical particle with a uniform layer of hydration product formed on its surface and gradually thickening [55,56]. Although analytically tractable and giving an expression for the rate of hydration in terms of particle dissolution rates and diffusion rates through the hydrated layer, these models were based on several unwarranted assumptions and were so idealized that they gave little insight into the underlying causes of the induction period or general trends in microstructure development where particle size distributions become important.

An alternative and currently popular theoretical approach is to employ phenomenological equations for nucleation and growth of C-S-H similar to those derived by Avrami [57], Johnson and Mehl [58], and Kolmogorov [59] to describe first order phase transformations in melts or single crystals. The main attraction of these models is their simplicity of application and ability to fit experimental calorimetry data in the vicinity of the main exothermic peak. However, there is a growing recognition that these models are based on underlying assumptions that are dubious at best when applied to cement hydration. Among these assumptions are that the thermodynamic driving force for the transformation is constant throughout the process, that the nucleating phase forms at random locations throughout the volume of the parent phase, and that diffusion is not required at any stage of the transformation. Consequently, these models cannot make any account of the induction period, solution chemistry or other microstructural detail, and their fits to experimental calorimetry data break down shortly following the main alite hydration exotherm. Thomas has removed at least the assumption of random nucleation in his recent boundary nucleation and growth model [60] by forcing C-S-H to nucleate only on the surface of C3S particles and has therefore been able to fit calorimetry data to somewhat longer times.

Beginning with the seminal work of Jennings and Johnson in 1986 [61], attention turned to modeling more realistic microstructures of cement paste, and these have now become powerful tools for understanding and predicting the development of mechanical and transport properties in these materials. The CEMHYD3D simulation model [62] developed at the National Institute of Standards and Technology (NIST) is the best-known and most widely used of these models. In CEMHYD3D, the 3D microstructure of cement paste is represented on a discretized lattice, capturing realistic particle size and shape distributions, the volume fraction and surface area fractions of the initial phases, and the spatial distribution of those phases (figure 8). Changes to the microstructure are simulated through a large set of rules that are evaluated locally at each lattice site, and that depend on the materials involved in the reaction. The resulting hydrated microstructures have a realistic appearance, quantitatively reasonable spatial distribution of phases, and realistic topology of capillary porosity down to a minumum pore size of 1 μm. Other properties that can be followed with CEMHYD3D are the heat evolution, chemical shrinkage, phase percolation and setting. The main limitations of CEMHYD3D are that its rules are not formulated to provide an inherent time scale to the changes that occur, and that the intimate relation between solution chemistry and the thermodynamics and kinetics of the coupled reactions is not modeled. These limitations render CEMHYD3D poorly suited to examine detailed mechanisms of hydration and the role of chemical additives in modifying the reaction rates by selective adsorption or other subtle mechanisms, although it is still a quite powerful tool for tracking general features of hydration that depend on microstructure.
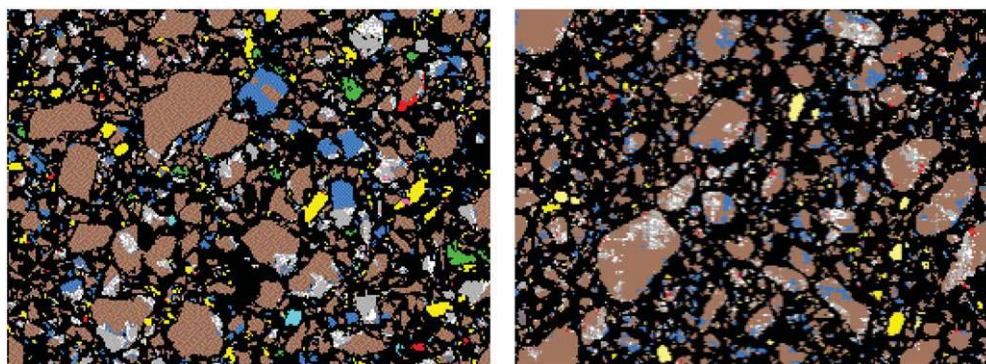
Fig. 8 (Left) SEM false color segmented image of a PC (sample 152 from the Cement and Concrete Reference Laboratory Proficiency Sample program). (Right) 2D slice from a 3D reconstruction of the same cement with a slightly lower packing fraction of particles. The phases are colored as follows: brown = C3S, blue = C2S, gray = C3A, white = C4AF, yellow = gypsum, red = arcanite, green = $CaCO_3$, cyan = quartz.

To address these limitations, a kinetic cellular automaton model has been developed at NIST to simulate the chemical kinetics of coupled reactions among solids in heterogeneous aqueous suspensions [63–65]. This model has been applied recently to examine microstructural development and solution chemistry during C3S hydration [66,67]. In the absence of unequivocal evidence supporting either the MBL hypothesis or the SDS hypothesis of the induction period, the model was used to examine the plausibility and implications of each hypothesis. The results showed that, no matter which of the two hypotheses is chosen, only heterogeneous nucleation of C-S-H on C3S surfaces can account for experimental observations of the evolution of the solution composition and degree of hydration in Stages 1 through 3. Those simulations also differentiated between heterogeneous nucleation and growth of C-S-H, and indicated that nucleation occurs in a fairly short burst over only a few minutes, either at the end of Stage 0 when assuming the SDS hypothesis or near the beginning of Stage 3 when assuming the MBL hypothesis. The narrow window of C-S-H nucleation occurs in the simulations because nucleation consumes calcium and especially silicates from solution, thus lowering the saturation index of C-S-H enough that the thermodynamic driving force for continued precipitation becomes less than the energetic barrier to nucleation.

These basic insights about the timing, location, and rates of nucleation and growth of C-S-H still provide no clear way to differentiate between the MBL and SDS hypotheses, and yet a better knowledge of the trigger for ending the induction period could have important consequences for designing chemical additives that control setting time. Therefore, subsequent uses of the model have investigated whether one hypothesis or the other makes distinguishable predictions about the influence of different mineral phases on the kinetics of C3S hydration. The investigation focused on the role of portlandite because (1) it is the only other major product of C3S hydration other than C-S-H, (2) portlandite is often observed to first precipitate near the end of the induction period, and (3) once formed, portlandite acts as a buffer controlling the calcium concentration in solution. In fact, the close correlation between portlandite formation and the end of the induction period has led some researchers to propose that portlandite precipitation actually causes the end of the induction period. Motivated by this, the model was used to test both the MBL and SDS hypotheses in simulations where portlandite was artificially prevented from forming.

The simulation results revealed a significant difference in behaviors depending on which hypothetical mechanism governs the induction period. Figure 9 shows the predicted degree of hydration (i.e. mass fraction of C3S consumed) as a function of time for three different scenarios. In the first simulation (open circles in figure 9), the SDS hypothesis was used to simulate normal hydration of C3S in water without any restriction on portlandite precipitation. In the second simulation, (open squares in figure 9), the SDS hypothesis was used to simulate hydration of the same system except that portlandite was not allowed to precipitate. Finally, a third simulation (open diamonds in figure 9) was identical to the second simulation except that the MBL hypothesis was used in place of the SDS hypothesis. The figure clearly shows a distinct difference in the effect of suppressing portlandite. When the SDS mechanism is operative, suppressing portlandite has a strong retarding effect on hydration; the induction period is prolonged by about 10 hours before a weak accelerating period begins. However, when the MBL mechanism is operative, there is no measurable retarding effect. The length of the induction period is
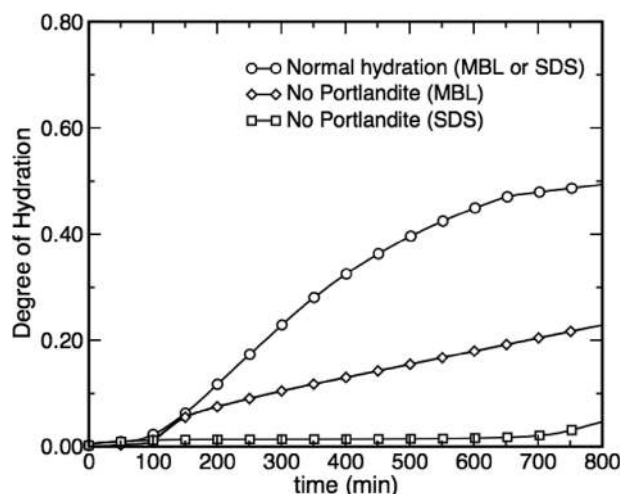
Fig. 9 Simulated rates of hydration of C3S as a function of time using NIST's kinetic cellular automaton model, testing the influence of the MBL and SDS hypothesis on changing the kinetics when the precipitation of portlandite is suppressed

virtually the same as in the control simulation, although the acceleration period which follows is shorter and a period of steady but slower hydration ensues.

The underlying reason for the differences in retarding effect is the higher calcium concentrations in solution when portlandite is not able to precipitate. Under the SDS hypothesis, much higher calcium concentrations force the silicate concentration to lower values, on the order of 0.1 μmol/L to maintain a near-equilibrium condition with C3S. The lower silicate concentrations result in a lower driving force for C-S-H growth. Therefore, neither the dissolution rate of C3S nor the growth rate of C-S-H is as great when portlandite cannot form and the induction period is extended. However, the situation is much different under the MBL hypothesis. When a metastable layer of hydrate protects highly soluble C3S from dissolving, this layer is destabilized by the formation of C-S-H, which happens early in the induction period. The destruction of the metastable layer causes renewed dissolution of C3S, and the higher calcium concentrations in solution due to the absence of portlandite has virtually no effect on the rate of dissolution of C3S because its solubility product is so high. Similarly, the silicate concentration is not reduced as much because it continues to be supplied to solution by C3S dissolution, and C-S-H can continue to grow. Therefore, neither the induction period nor the beginning of the acceleration period is noticeably affected by suppressing portlandite when the MBL mechanism is operative. Incidentally, we remark that the apparent reason for the shortening of the acceleration period under the MBL hypothesis is a continual re-formation and dissolution of the metastable hydrate at the C3S surfaces, which provides partial protection and decrease of the C3S dissolution rate. We cannot yet confirm that this latter effect is realistic, although Gartner has proposed a similar effect in an earlier review [68].

Another area, directly related to adsorption and crystal growth phenomena in cement, where these kinds of models can provide useful insight and guidance is in understanding the influence of calcium sulfate in controlling the rate of hydration of Portland cement and pozzolanic cement (defined in Table 2). Since the seminal study by Tenoutasse in 1968 [69] it has been recognized that C3S hydration is strongly retarded in Portland cements where the sulfate content is insufficient to promote complete conversion of C3A to ettringite. Likewise, the presence of calcium sulfate in solution is known to mildly retard the hydration of pure C3S pastes [70]. However, a compelling mechanistic explanation of these admixture effects has not been given. Indeed, these admixture effects seem unusual at first because sulfate species do not participate in the reactions for simple C3S dissolution or growth of C-S-H or portlandite. A key to understanding these admixture effects may be to understand whether selective adsorption of ions occurs at reactive surface sites of clinker minerals or hydration products.

Recently, nanoscopic surface techniques such as atomic force microscopy (AFM) or vertical scanning inter-ferometry (VSI), along with molecular-scale kinetic Monte Carlo or molecular dynamics simulations have been used to elucidate the mechanisms of interaction between adsorbates and mineral surfaces [71], and these same techniques may eventually be applied to sulfate interactions with cement. Even so, the kinetic cellular automaton
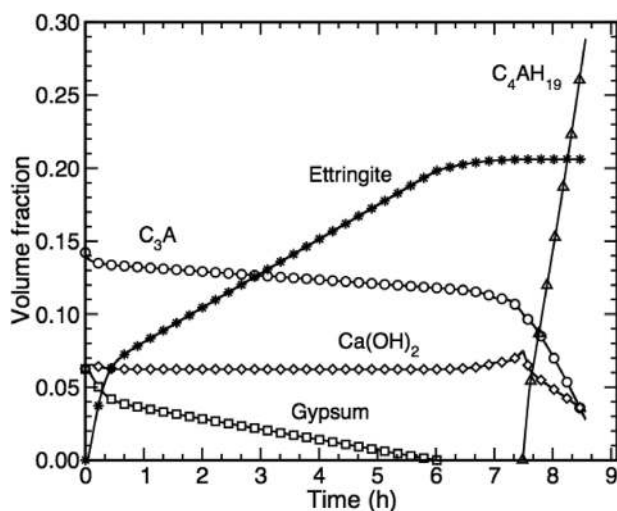
Fig. 10 Time dependence of solid phases during a kinetic cellular automaton simulation of hydration of the C3A-gypsum-portlandite system.
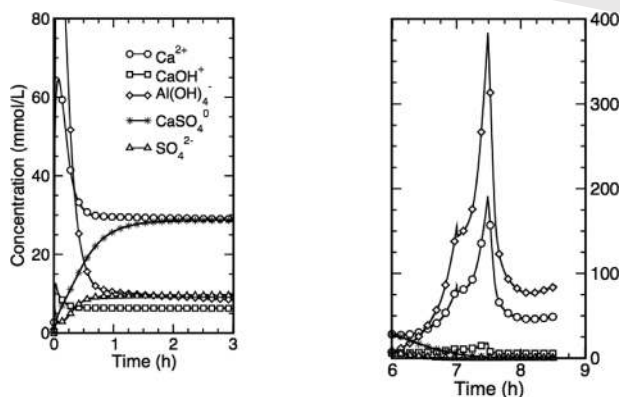
Fig. 11 Evolution of the solution composition for the simulation of hydration of the C3A-gypsum-portlandite system depicted in Fig. 10.

approach can be used now to begin analyzing some possible mechanisms by which sulfates alter hydration kinetics.

A random particulate microstructure in water was created with C3A, gypsum, and portlandite particles, with the initial volume fractions being 0.14, 0.06, and 0.06, respectively. The portlandite was added because its influence in buffering the calcium concentration in cement provided solution compositions that are similar to those in low-alkali Portland cement pastes. The only reactions that were assumed were the congruent, reversible dissolution/growth of gypsum, portlandite, C3A, ettringite, calcium monosulphoaluminate, and the hexagonal C4AH19 phase. In addition, the solution speciation reactions for formation of $CaOH^+$ and $CaSO_4^0$ complexes were assumed. Stoichiometries and equilibrium constants for these reactions were taken from standard thermochemical databases [35,36]. Finally, the reversible adsorption of $CaSO_4^0$ on active dissolution sites of C3A was also assumed, as suggested by Minard [72]. This adsorption reaction is assumed to slow the rate of C3A dissolution in proportion to the surface concentration of the adsorbate, and is the only plausible mechanism that has been proposed to explain the rapid reduction in dissolution rates of C3A that occurs at solution concentrations far below the saturation point. Nevertheless, direct evidence for adsorption reaction is lacking and in the absence of experimental data, we have assumed that it involves the single-step attachment of $CaSO_4^0$ on the surface, with an equilibrium constant of 10^{-4}.

Figure 10 shows the simulated changes in the volume fraction of all the solid phases as a function of time, and figure 11 shows the change in solution composition for the same system. The dissolution of C3A is initially

very rapid, consistent with its high solubility, but decreases within about 10 min to a steady value as indicated by the constant rate of decrease in the C3A volume fraction. Likewise, gypsum also dissolves fairly rapidly at the beginning but slows to a steady state value. Ettringite, $[Ca_3Al(OH)_6 \cdot 12H_2O]_2 \cdot (SO_4)_3 \cdot 2H_2O$, a very sparingly soluble mineral, nucleates and grows rapidly almost as soon as C3A and gypsum begin dissolving, but once again reaches a steady state value for several hours afterward. Between 10 min and 6 h, the kinetics of the system is controlled by the dissolution of C3A, which is slowed by the initial adsorption of $CaSO_4^0$. Ettringite grows at a steady rate governed by the rate at which aluminate ions are made available in solution by the dissociation of C3A, and gypsum dissolves at a rate that keeps it in equilibrium with the solution as sulfate ions are consumed by ettringite formation. During this time interval, the solution composition is nearly constant (figure 11). However, this kinetic behavior begins to change once all of the gypsum is consumed at about 6 h. When this happens, ettringite continues to grow for about another hour, although its rate steadily decreases because the continual reduction in sulfate concentration reduces the driving force for ettringite growth (see right panel of figure 11). In addition, when the ettringite has removed most of the remaining sulfates from solution, sulfates adsorbed on C3A spontaneously desorb by Le Chatelier's principle. When this happens, the dissolution rate of C3A sharply increases shortly after 7 h have elapsed. The renewed dissolution rapidly increases the concentrations of calcium, aluminates, and hydroxyls in solution (see right panel of figure 11). C4AH19 nucleates and rapidly grows in this solution, causing the concentrations of these species to be reduced somewhat.

As already described, the general trends in the dissolution of C3A shown in figure 10 are typically observed experimentally in the C3A-gypsum system [68]. It had long been thought that the initial decrease in C3A dissolution rate was caused by the formation of a layer of ettringite around the C3A particles which, like the hypothetical metastable hydrate in the C3S system, partially sealed the particles off from the solution. The renewal of C3A dissolution at later times was thought to be due to a transformation of the ettringite layer to a more porous calcium mono-sulfoaluminate, the latter phase being thermodynamically preferred to ettringite once sulfates have been removed from solution. However, an abundance of microscopic evidence suggests that ettringite forms as rather shortened needles nearby, but not on, the C3A particle surfaces, and it is difficult to see how these needles could form a protective layer. More importantly, recent experimental work has shown that the transformation from ettringite to calcium mono-sulfoaluminate happens quite slowly, perhaps over a few days time [72]. The current simulations are consistent with this observation, for even though calcium monosulfoaluminate is able to form in the simulations, it is never observed to do so for as long as three hours after the sulfates have been removed from the solution by ettringite. In any event, the transformation from ettringite to calcium monosulfoaluminate is unlikely to occur rapidly enough to account for the rapid change in C3A dissolution rates at later times.

In cement technology jargon, one would say that the system just discussed was "undersulfated" because the gypsum was consumed before all the C3A reacted. A basic stoichiometric analysis suggests that a 3:1 molar ratio of gypsum:C3A (or, equivalently, a 5:2 volume ratio) is required to allow complete conversion to ettringite. In contrast, the system simulated here, which was formulated to mimic one reported by Gartner [68], had only a 3:7 volume ratio.

In the C3S-C3A-gypsum system, which is similar to Portland cement, an undersulfated condition causes the formation of hexagonal aluminate hydrates like C4AH19, just as seen in these simulations, but it also causes the acceleration period of C3S dissolution to be both delayed and substantially weakened [69], The result is a severe retardation and delay of setting in undersulfated Portland cements. The reason for this effect is not clear. It is known that aluminates can substitute for silicates in the "drierketten" silicate chains if the aluminate concentration in solution is sufficiently high. It has been speculated that an undersulfated condition causes an elevation in aluminate concentrations, similar to those observed at later times in figure 11, and that the aluminate substitution in C-S-H causes a significant reduction in its growth rate [73]. This argument seems plausible, although direct experimental evidence of a significant dependence of the growth rate of C-S-H on its composition has not been obtained. Another proposal is that the hexagonal aluminate hydrates, which form so rapidly and abundantly in the absence of sulfates, effectively fill the pore space to such an extent that there is no room left for C-S-H to grow [74]. Because there is strong evidence that C-S-H growth controls the rate of hydration of C3S, as discussed earlier, this argument also seems plausible. Again, however, direct experimental evidence of space filling by an aluminate hydrate in undersulfated cement paste is sparse.

The undersulfation problem in Portland cement is so well known that it is common practice to determine the "optimum" sulfate level for a Portland cement clinker. The optimum sulfate level is determined not just by the aluminate stoichiometry, but also seems to be influenced by other factors such as the surface area (fineness) of the cement particles, as well as the distribution and polymorphic form of the clinker phases. Therefore, the determination of optimum sulfate levels is often made by trial and error experimentation, using

isothermal calorimetry to detect the timing and strength of the main C3S hydration peak, and then inter-grinding this concentration of gypsum to make the Portland cement. Unfortunately, this same sulfate level is unlikely to be optimal for the same Portland cement with partial replacement by fly ash or other pozzolanic materials, because these latter materials themselves often contain calcium aluminates in the form of crystals or reactive glassy phases. Under-sulfated conditions in these blended cements often leads to what concrete technologists call "incompatibility", which is a failure to set. Because of its importance in effectively utilizing sustainable concrete materials and because of the cumbersome trial-and-error experimental methods that are required to determine optimum sulfate levels in these materials, one major objective of this kind of computer modeling research is to provide a tool that can help predict the optimum sulfate level for any cement composition.

7   Summary

The hydration of cement paste is responsible for the development of essentially every engineering property of concrete, including, but not limited to, setting and hardening, temperature rise in massive concrete structures, autogenous shrinkage that can lead to cracking, and resistance to leaching, sulfate attack and other degradation phenomena. This fact provides a high motivation to understand the fundamental mechanisms of cement hydration with the aim of controlling the properties of interest in a given situation. Progress in this area has been hindered by the significant complexity of the hydration process, from the points of view of chemistry, kinetics, and microstructure development. This chapter has discussed various aspects of these complexities from the point of view of the impact of adsorption and crystal growth phenomena. Recent advances in experimental techniques [75] and computational modeling [76] are beginning to provide a more basic understanding of these processes in cement paste, but there are still a large number of unanswered questions that will require sustained interdisciplinary research efforts well into the future.

References

[1]   R. G. Blezard, in: The History of Calcareous Cements, edited by P. C. Hewlett, Lea's Chemistry of Cement and Concrete, 4th Edition (Butterworth-Heimann, Oxford, 1998), pp. 1–23.

[2]   A. Bentur, Cementitious materials – Nine millennia and a new century: Past, present, and future. American Society of Civil Engineers, 150th Anniversary Paper. J. Mater. Civ. Eng., JAN/FEB 2002, pp. 2–22.

[3]   H. F. W. Taylor, Cement chemistry. 2nd Edition. (Thomas Telford, London, 1997).

[4]   E. M. Gartner, J. F. Young, D. A. Damidot, and I. Jawed, Hydration of Portland cement, in: J. Bensted, P. Barnes (Eds.), Structure and Performance of Cements, 2nd ed. (Spon Press, London – New York, 2002), pp. 57–113.

[5]   I. Odler (ed.), Special Inorganic Cements (Spon Press, London – New York, 2000).

[6]   A. K. Chatterjee, in Special Cements, edited by J. Bensted, P. Barnes, Structure and Performance of Cements, 2nd ed. (Spon Press, London – New York, 2002), pp. 186–236.

[7]   G. Artioli, Scientific methods and cultural heritage (Oxford University Press, Oxford, 2010).

[8]   V. S. Ramachandran, V. M. Malhotra, C. Jolicoeur, and N. Spiratos, Superplasticizers: properties and applications in concrete (CANMET, Materials Technology Laboratory, Ottawa, 1998).

[9]   R. Rixom and N. Mailvaganam, Chemical Admixtures for Concrete, 3rd ed. (E & FN Spon, London, 1999).

[10] S. Chandra, in: Properties of Concrete with Mineral and Chemical Admixtures, edited by J. Bensted, P. Barnes, Structure and Performance of Cements, 2nd ed. (Spon Press, London – New York, 2002), pp. 140–185.

[11] K. Van Breugel, Cem. Concr. Res. **34**, 1661 (2004).

[12] H. M. Jennings and P. L. Pratt, Cem. Concr. Res. **9**, 501 (1979).

[13] E. M. Gartner and H. M. Jennings, J. Am. Ceram. Soc. **80**, 743 (1987).

[14] R. A. Livingston, J. S. Schweitzer, C. Rolfs, H. W. Becker, and S. Kubsky, J. Mater. Res. **16**, 687 (2001).

[15] J. S. Schweitzer, R. A. Livingston, C. Rolfs, H. W. Becker, S. Kubsky, T. Spillane, M. Castellote, and P. G. de Viedma, Nucl. Instrum. Meth. Phys. Res. **B 241**, 441 (2005).

[16] S. Garrault and A. Nonat, Langmuir **17**, 8131 (2001).

[17] S. Garrault-Gauffinet and A. Nonat, J. Cryst. Growth **200**, 565 (1999).

[18] S. Garrault, E. Finot, E. Lesniewska, and A. Nonat, Mater. Structures **38**, 435 (2005).

[19] A. Nonat (ed.) Hydration and Setting. Why Does Cement Set? An Interdisciplinary Approach, Proc. 2nd International RILEM Symposium (PRO13, RILEM Publications, Cachan, 2000).

[20] R. J. Flatt, Mat. Struct. **37**, 289 (2004).

[21] F. Cella, T. Cerulli, D. Salvioni, and S. Stella, Morphological variation of cement paste microstructure due to the use of admixtures. Proceedings of the 23th International Conference on Cement Microscopy, pp. 117–136, (2001).

[22] C. Rößler, A. Eberhardt, H. Kucerova, and B. Moser, Cem. Concr. Res. **38**, 897 (2008).

[23] C. Rößler and J. Stark, in: The Influence of Superplasticizers on the Microstructure Development in Normal Portland Cement and C3S, edited by P. C. Nkinamubanzi, Seventh CANMET/ACI International Conference on Superplasticizers and other Chemical Admixtures in Concrete in Berlin, Supplementary papers, pp. 17–32, (2003).

[24] E. Sakai, K. Yamada, and A. Ohta, J. Adv. Concr. Techn. **1**, 16 (2003).

[25] J. L. W. Griffin, P. V. Coveney, A. Whiting, and R. Davey, J. Chem. Soc. Perkin Trans. **2**, 1973 (1999).

[26] X. Zhang, W. Chang, T. Zhang, and C. K. Ong, J. Am. Ceram. Soc. **83**, 2600 (2000).

[27] A. J. Allen, J. J. Thomas, and H. M. Jennings, Nature Materials **6**, 311 (2007).

[28] J. Skibsted and C. Hall, Cem. Concr. Res. **38**, 205 (2008).

[29] E. Bonaccorsi, S. Merlino, and A. R. Kampf, J. Am. Ceram. Soc. **88**, 505 (2005).

[30] E. Bonaccorsi, S. Merlino, and H. F. W. Taylor, Cem. Concr. Res., **34**, H. F. W. Taylor Commemorative Issue, 1481 (2004).

[31] I. G. Richardson, Cem. Concr. Res. **34**, H. F. W. Taylor Commemorative Issue, 1733 (2004), See also I. G. Richardson, Electron Microscopy of Cements, in: Structure and performance of cements, edited by J. Bensted, P. Barnes, 2nd ed. (Spon Press, London – New York), pp. 500–556, (2002).

[32] I. G. Richardson, Cem. Concr. Res. **38**, 137 (2008).

[33] A. Popova, G. Geoffroy, M.-F. Renou-Gonnord, P. Faucon, and E. Gartner, J. Am. Ceram. Soc. **83**, 2556 (2000).

[34] J. J. Beaudoin, H. Dramé, L. Raki, and R. Alizadeh, Mater. Struc. **42**, 1003 (2009).

[35] D. L. Parkhurst, User's guide to PHREEQC-a computer program for speciation reaction-path, advective-transport, and geochemical calculations, Water-Resources Investigations Report 95–4227, U.S. Geological Survey, (1995).

[36] W. Hummel, U. Berner, E. Curti, F. J. Pearson, and T. Thoenen, Nagra / PSI Chemical Thermodynamic Data Base 01/01 (Universal Publishers, Parkland, Florida, 2002).

[37] S. Garrault and A. Nonat, Langmuir **17**, 8131 (2001).

[38] H. N. Stein, Cem. Concr. Res. **2**, 167 (1972).

[39] S. Gauffinet, E. Finot, R. Lesniewska, and A. Nonat, Earth Planet. Sci. **327**, 231 (1998).

[40] A. J. Allen, R. C. Oberthur, D. Pearson, P. Schofield, and C. R. Wilding, Phil. Mag. **B 56**, 263 (1987).

[41] H. M. Jennings, Cem. Concr. Res. **30**, 101 (2000).

[42] J. J. Thomas, H. M. Jennings, and J. J. Chen, J. Phys. Chem. **C 113**, 4327 (2009).

[43] N. Meller, K. Kyritsis, and C. Hall, Cem. Concr. Res. **39**, 45 (2009).

[44] J. R. Houston, R. S. Maxwell, and S. A. Carroll, Geochem. Trans. **10**, 1 (2009).

[45] A. Nonat, Cem. Concr. Res. **34**, 1521 (2004).

[46] H. M. Jennings, Cem. Concr. Res. **38**, 275 (2008).

[47] X. Cong and R. J. Kirkpatrick, Advn. Cem. Bas. Mater. **3**, 133 (1996).

[48] F. Brunet, Ph. Bertani, Th. Charpentier, A. Nonat, and J. Virlet, J. Phys. Chem. **B 108**, 15494 (2004).

[49] A. N. Christensen, N. V. Y. Scarlett, I. C. Madsen, T. R. Jensen, and J. C. Hanson, Dalton Trans. 1529 (2003).

[50] M. Merlini, G. Artioli, T. Cerulli, F. Cella, and A. Bravo, Cem. Concr. Res. **38**, 477 (2008).

[51] T. R. Jensen and A. N. Christensen, J. C. Cem. Concr. Res. **35**, 2300 (2005).

[52] G. Artioli, T. Cerulli, G. Cruciani, M. C. Dalconi, G. Ferrari, M. Parisatto, A. Rack, and R. Tucoulou, Anal. Bioanal. Chem. **397**, 2131 (2010).

[53] H. Manzano, A. Ayuela, and J. S. Dolado, J. Computer-Aided Mater. Des. **14**, 45 (2007).

[54] S. Bishnoi and K. L. Scrivener, Cem. Concr. Res. **39**, 266 (2009).

[55] R. Kondo, and S. Ueda, in: Kinetics and Mechanisms of the Hydration of Cements, edited by Proceedings of the Fifth International Symposium on the Chemistry of Cement, Vol. II (Tokyo, Japan, 1968), pp. 203–248.

[56] J. M. Pommersheim and J. R. Clifton, Cem. Concr. Res. **9**, 765 (1979).

[57] M. Avrami, J. Chem. Phys. **7**, 1103 (1939).

[58] W. A. Johnson and R. F. Mehl, Trans. Am. Inst. Min. (Metall.) Eng. **135**, 416 (1939).

[59] A. N. Kolmogorov, Bull. Acad. Sci. USSR Phys. Ser. **1**, 255 (1937).

[60] J. J. Thomas, J. Am. Ceram. Soc. **90**, 3282 (2007).

[61] H. M. Jennings and S. K. Johnson, J. Am. Ceram. Soc. **69**, 790 (1986).

[62] D. P. Bentz, J. Am. Ceram. Soc. **80**, 3 (1997).

[63] J. W. Bullard, Modelling Simul. Mater. Sci. Eng. **15**, 711 (2007).

[64] J. W. Bullard, J. Phys. Chem. **A 111**, 2084 (2007).

[65] J. W. Bullard, E. Enjolras, W. L. George, S. G. Satterfield, and J. E. Terrill, Modelling Simul. Mater. Sci. Eng. **18**, 025007 (2010).

[66] J. W. Bullard, J. Am. Ceram. Soc. **91**, 2088 (2008).

[67] J. W. Bullard and R. J. Flatt, J. Am. Ceram. Soc. **93**, 1894 (2010).

[68] E. M. Gartner, J. M. Gaidis, in: Hydration Mechanisms, edited by J. Skalny, Materials Science of Concrete, Amer. Ceramic Soc. (Westerville, OH, 1989), pp. 95–125.

[69] N. Tenoutasse, in: The Hydration Mechanism of C3A and C3S ins the Presence of Calcium Chloride and Calcium Sulfate, edited by Proceedings of the Fifth International Symposium on the Chemistry of Cement Vol. II (Tokyo, Japan, 1968), pp. 372–378.

[70] P. W. Brown, C. L. Harner, and E. J. Prosen, Cem. Concr. Res. **16**, 17 (1985).

[71] J. Cama, L. Zhang, G. De Giudici, J. M. Soler, R. S. Arvidson, and A. Luttge, Geochim. Cosmochim. Acta **73**, A187 (2009).

[72] H. Minard, S. Garrault, L. Regnaud, and A. Nonat, Cem. Concr. Res. **37**, 1418 (2007).

[73] S. Garrault, H. Minard, and A. Nonat, in: Hydration of Silicate Phase and Mechanical Evolution in "Alite-Tricalcium Aluminate-gypsum" Complex System, edited by J. Beaudoin, Proceedings of the 12th International Congress on the Chemistry of Cement (Montreal, Canada, 2007), pp. TH6–08.1.

[74] K. Scrivener, personal communication, (2009).

[75] J. W. Bullard, H. M. Jennings, R. A. Livingston, A. Nonat, G. W. Scherer, J. S. Schweitzer, K. L. Scrivener, and J. J. Thomas, Cem. Concr. Res. **41**, 1208 (2011).

[76] J. J. Thomas, J. J. Biernacki, J. W. Bullard, S. Bishnoi, J. S. Dolado, G. W. Scherer, and A. Luttge, Cem. Concr. Res. **41**, 1257 (2011).

USING e-ANNOTATION TOOLS FOR ELECTRONIC PROOF CORRECTION

**Required software to e-Annotate PDFs: <u>Adobe Acrobat Professional</u> or <u>Adobe Reader</u> (version 8.0 or above). (Note that this document uses screenshots from <u>Adobe Reader X</u>)**
The latest version of Acrobat Reader can be downloaded for free at: <u>http://get.adobe.com/reader/</u>

Once you have Acrobat Reader open on your computer, click on the Comment tab at the right of the toolbar:

| | | | | | 1 | / 27 | | | 70.4% | | | | | Tools | Comment | Share |

This will open up a panel down the right side of the document. The majority of tools you will use for annotating your proof will be in the Annotations section, pictured opposite. We've picked out some of these tools below:

▾ **Annotations**

---
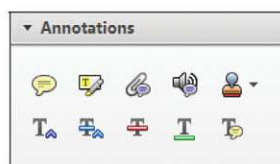
1. Replace (Ins) Tool – for replacing text.
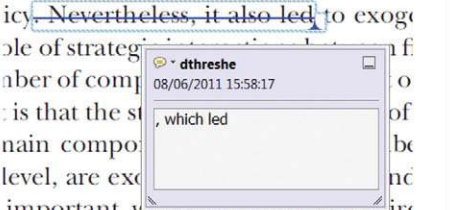
Strikes a line through text and opens up a text box where replacement text can be entered.

How to use it

- Highlight a word or sentence.
- Click on the Replace (Ins) icon in the Annotations section.
- Type the replacement text into the blue box that appears.

idard framework for the analysis of m
icy. Nevertheless, it also led to exoge
ole of strategic~~n~~ ~~n~~ f
nber of comp
 is that the st
nain compo
level, are ex
important ~~works~~ ~~on~~ ~~entry~~ ~~by~~
M henceforth)[1] we open the 'black l

dthreshe
08/06/2011 15:58:17

, which led

---

2. Strikethrough (Del) Tool – for deleting text.

Strikes a red line through text that is to be deleted.

How to use it

- Highlight a word or sentence.
- Click on the Strikethrough (Del) icon in the Annotations section.

there is no room for extra profits a
 ups are zero and the number of
 <et) values are not determined by
 Blanchard ~~and Kiyotaki~~ (1987),
 rfect competition in general equili
 ts of aggregate demand and supply
 lassical framework assuming mono
 een an exogenous number of firms

---

3. Add note to text Tool – for highlighting a section to be changed to bold or italic.
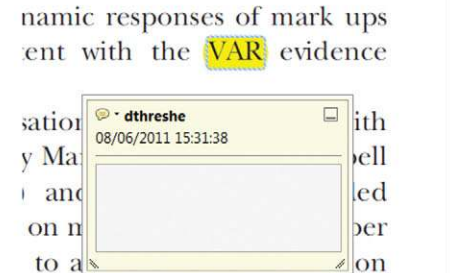
Highlights text in yellow and opens up a text box where comments can be entered.

How to use it

- Highlight the relevant section of text.
- Click on the Add note to text icon in the Annotations section.
- Type instruction on what should be changed regarding the text into the yellow box that appears.

namic responses of mark ups
ent with the `VAR` evidence

sation
y Ma
 and
on m
to a
stent also with the demand-

dthreshe
08/06/2011 15:31:38

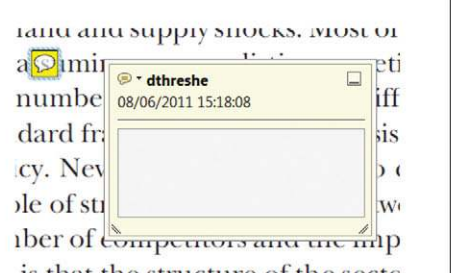### 4. Add sticky note Tool – for making notes at specific points in the text.

Marks a point in the proof where a comment needs to be highlighted.

How to use it

- Click on the Add sticky note icon in the Annotations section.
- Click at the point in the proof where the comment should be inserted.
- Type the comment into the yellow box that appears.

land and supply shocks. Most of
a<umi
numbe
dard fr
icy. Nev
ole of st
nber of competitors and the imp
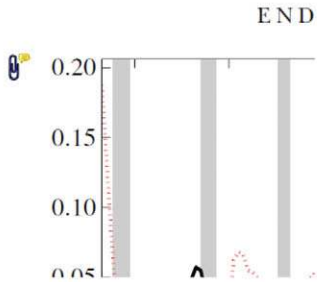 is that the structure of the secto

dthreshe
08/06/2011 15:18:08

USING e-ANNOTATION TOOLS FOR ELECTRONIC PROOF CORRECTION

5. Attach File Tool – for inserting large amounts of text or replacement figures.

Inserts an icon linking to the attached file in the appropriate pace in the text.

How to use it

- Click on the Attach File icon in the Annotations section.
- Click on the proof to where you'd like the attached file to be linked.
- Select the file to be attached from your computer or network.
- Select the colour and type of icon that will appear in the proof. Click OK.

6. Add stamp Tool – for approving a proof if no corrections are required.

Inserts a selected stamp onto an appropriate place in the proof.

How to use it

- Click on the Add stamp icon in the Annotations section.
- Select the stamp you want to use. (The Approved stamp is usually available directly in the menu that appears).
- Click on the proof where you'd like the stamp to appear. (Where a proof is to be approved as it is, this would normally be on the first page).
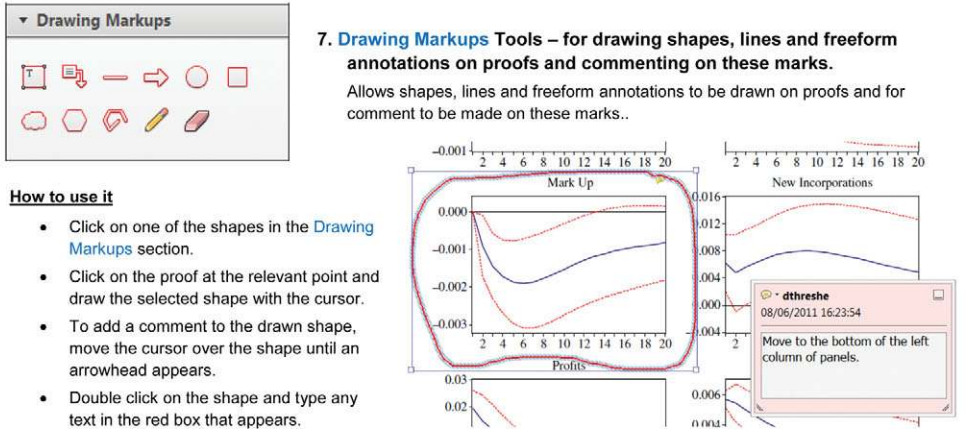
7. Drawing Markups Tools – for drawing shapes, lines and freeform annotations on proofs and commenting on these marks.

Allows shapes, lines and freeform annotations to be drawn on proofs and for comment to be made on these marks..

How to use it

- Click on one of the shapes in the Drawing Markups section.
- Click on the proof at the relevant point and draw the selected shape with the cursor.
- To add a comment to the drawn shape, move the cursor over the shape until an arrowhead appears.
- Double click on the shape and type any text in the red box that appears.

For further information on how to annotate proofs, click on the Help menu to reveal a list of further options:
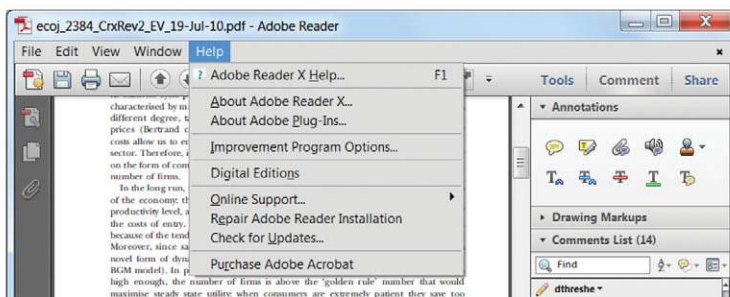
Instructions for Proof Corrections and Orders

Please correct your proofs and return them within 3 days together with the completed reprint order form. The editors reserve the right to publish your article with editors' corrections if your proofs do not arrive in time.

After having received your corrections, your paper will be published online soon in the Wiley Online Library (wileyonlinelibrary. com).

Please keep in mind that reading proofs is your responsibility. Corrections should therefore be clear. We prefer the corrections be made directly within the PDF file (see E-annotations instructions). Alternatively, you may provide us with a list of corrections by e-mail, with the corrections referring to their line number.

Manuscript files are sometimes slightly modified by the production department to follow general presentation rules of the journal.

Check the enclosed proofs very carefully, paying particular attention to the formulas (including line breakings introduced in production), figures, numerical values, tabulated data and layout of the pages.

A black box (■) or a question at the end of the paper (after the references) signals unclear or missing information that specifically requires **your attention.** Note that the author is liable for damages arising from incorrect statements, including misprints.

The main aim of proofreading is to correct errors that may have occurred during the production process, **and not to modify the content of the paper**. Corrections that may lead to a change in the page layout should be avoided.

Note that sending back a corrected **manuscript** file **is of no use**.

Return the corrected proofs within 3 days by e-mail.

Please do not send your corrections to the typesetter but to the Editorial Office:

E-MAIL Crystal-Research@wiley.com

Please limit corrections to errors in the text; cost incurred for any further changes or additions will be charged to the author, unless such changes have been agreed upon by the editor.

Full color reprints, Customized PDF files, Printed Issues, and Cover Posters may be ordered by filling in the accompanying form.

Contact the Editorial Office for **special offers** such as

- Personalized and customized reprints (e.g. with special cover, selected or all your articles published in Wiley-VCH journals)
- Cover/frontispiece publications and posters (standard or customized)
- Promotional packages accompanying your publication

Visit the **MaterialsViews.com Online Store** for a wide selection of posters, logos, prints and souvenirs from our top physics and materials science journals at www.cafepress.com/materialsviews

Order Form

Crystal Research and Technology

2013

WILEY-VCH Verlag GmbH & Co. KGaA
Crystal Research and Technology
Rotherstrasse 21
10245 Berlin
Germany

TEL +49 (0) 30–47 03 13 38
FAX +49 (0) 30–47 03 13 99
E-MAIL Crystal-Research@wiley.com

WILEY *Publishers Since 1807*

Article No.

Author/Title

e-mail address

Please complete this form and return it by e-mail or FAX.

Required Fields may be filled in using Adobe Reader

Reprints/Issues/PDF Files/Posters

Whole issues (printed on demand), reprints and PDF files (300 dpi) for an unlimited number of printouts are available at the rates given on the next page. Reprints and PDF files can be ordered before *and after* publication of an article. All reprints will be delivered in full color.

Reprints

Please send me and bill me for

☐ full color reprints with color cover

☐ full color reprints with personalized color cover

Issues (printed on demand)

Please send me and bill me for

☐ 5 entire issues ☐ 10 entire issues

☐ more than 10 entire issues (please contact the editorial office)

Customized PDF-Reprint

Please send me and bill me for

☐ a PDF file (300 dpi) for an unlimited number of printouts **with customized color cover sheet.**

The PDF file will be sent to your e-mail address.

Send PDF file to:

Please note that posting of the final published version on the open internet is not permitted. For author rights and re-use options, see the Copyright Transfer Agreement at http://www.wiley.com/go/ctavchglobal.

Cover Posters

Posters are available of all the published covers in two sizes (see attached price list). **Please send me and bill me for**

☐ A2 (42 × 60 cm/17 × 24in) posters
☐ A1 (60 × 84 cm/24 × 33in) posters

Mail reprints and/or issues and/or posters to (no P.O. Boxes):

VAT number:

Information regarding VAT

Please note that from German sales tax point of view, the charge for **Reprints, Issues or Posters** is considered as **"supply of goods"** and therefore, in general, such delivery is a subject to German sales tax. However, this regulation has no impact on customers located outside of the European Union. Deliveries to customers outside the Community are automatically tax-exempt. Deliveries within the Community to institutional customers outside of Germany are exempted from the German tax (VAT) only if the customer provides the supplier with his/her VAT number.

The VAT number (value added tax identification number) is a tax registration number used in the countries of the European Union to identify corporate entities doing business there. It starts with a country code (e.g. FR for France, GB for Great Britain) and follows by numbers.

The charge for **front cover/back cover/inside cover pictures, color figures or frontispieces publications** is considered as **"supply of services"** and therefore it is a subject to German sales tax. However, in case you are an institutional customer outside of Germany, the tax can be waived if you provide us with the VAT number of your company.

Customers outside of the EU may have a VAT number starting with "EU" instead of the country code if they are registered by the EU's tax authorities. In case you do not have a VAT number of EU and you are a taxable person doing business in a country outside EU, then please provide us with a certification from your local tax authorities confirming that you are a taxable person under the local tax law. Please note that the certification needs to confirm that you are a taxable person and you are conducting an economic activity in your country. Certifications which confirm that you are tax-exempt legal body (non-profit organization, public body, school, political party, etc.) in your country cannot be accepted for the German VAT purposes.

Purchase Order No.:

Terms of payment:

☐ Please send an invoice ☐ Cheque is enclosed

☐ **VISA, MasterCard and AMERICAN EXPRESS.**

Please use this link (Credit Card Token Generator) to create a secure Credit Card Token and include this number in the form instead of the credit card data.

https://www.wiley-vch.de/editorial_production/index.php

CREDIT CARD TOKEN NUMBER:

Send invoice to:

Signature _____

Date _____

Please use this form to confirm that you are prepared to pay your contribution.

Please sign and return this page.

You will receive an invoice following the publication of your article in the journal issue.

Price List – Crystal Research and Technology 2013

WILEY
Publishers Since 1807

Reprints/Issues/PDF-Files/Posters

The prices listed below are valid only for orders received in the course of 2013. Minimum order for reprints is 50 copies. **Reprints can be ordered before *and after* publication of an article. All reprints are delivered with color cover and color figures**. If more than 500 copies are ordered, special prices are available upon request.

Entire issues are available to authors at a reduced price.

The prices include mailing and handling charges. All prices are subject to local VAT/sales tax.

Reprints with color cover Size (pages)	Price for orders of (in Euro)					
	50 copies	100 copies	150 copies	200 copies	300 copies	500 copies*
1–4	345	395	425	445	548	752
5–8	490	573	608	636	784	1077
9–12	640	739	786	824	1016	1396
13–16	780	900	958	1004	1237	1701
17–20	930	1070	1138	1196	1489	2022
for every additional 4 pages	147	169	175	188	231	315
for personalized color cover	**190**	**340**	**440**	**650**	**840**	**990**

PDF file (300 dpi, unlimited number of printouts, customized cover sheet)	€ 330

Issues (printed on demand)	€ 48 per copy for up to 10 copies.**

Cover Posters
- A2 (42×60 cm/17×24in) € 49
- A1 (60×84 cm/24×33in) € 69

*Prices for more copies available on request.

**Minimum order is 5 copies.

Special offer: If you order 100 or more reprints you will receive a pdf file (300 dpi, unlimited number of printouts, color figures) for free.